2018 European Control Conference (ECC)
June 12-15, 2018. Limassol, Cyprus

State and Parameter Estimation for a Gas-Liquid Cylindrical Cyclone

Torstein Thode Kristoffersen* and Christian Holden*

***Abstract*— The development and production of hydrocarbons from oil and gas discoveries in deep water require cost-efficient compact separation technology. However, the small operational volume of compact separators make them highly sensitive to changes in flow rate and composition. Therefore, measurements of critical variables are crucial for providing operators with the necessary insight, as well as enabling the use of advanced controllers to efficiently control such separators. Available measurements are, however, often limited due to high investment cost or lack of suitable sensor technology. Estimators (soft sensors) can alleviate this problem. The gas-liquid cylindrical cyclone is a type of compact separator recently considered for subsea application. Several advanced controllers have recently been derived for this separator, but estimators are needed for implementation in subsea applications. Therefore, in this paper, we develop and study the performance of the UKF and MHE estimators providing state feedback to a linear MPC.**

I. INTRODUCTION

Today, most of the developed oil and gas discoveries are in shallow waters in areas near to shore, while recent oil and gas discoveries are in deep waters in remote areas. Subsea compact separation technology is a crucial component for the development and production of these recent discoveries. The compact design and low weight of these separators allow installation in deep waters, where traditional separators can not be used, enabling efficient single-phase boosting of gas and liquid at economically feasible costs [1].

The Gas-Liquid Cylindrical Cyclone (GLCC) separator (Fig. 1) is a type of compact separator recently considered for subsea applications [2] and has been successfully applied for a wide range of onshore applications [3]. The compact operational volume of these separators reduce the separation performance and robustness against changes in inlet flow rates and composition. Therefore, a challenging objective for the control system is to efficiently control the liquid level to ensure acceptable separation performance and stable operating conditions for downstream boosting equipment. Advanced control systems are required to handle the large variations in inlet flow rates and conditions, often requiring full knowledge of the states and parameters of the model applied by the controller.

Several issues arise for enabling operation of a subsea compact separation plant. Measurements of critical variables are crucial for providing operators with necessary insight, and for enabling use of advanced controllers to efficiently control such a plant. Available measurements are, however, often limited due to lack of suitable sensor technology,

* Department of Mechanical and Industrial Engineering, Norwegian University of Science and Technology (NTNU). torstein.t.k@gmail.com, christian.holden@ntnu.no

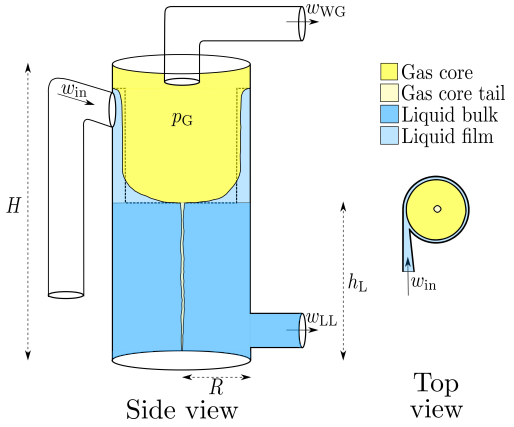

Fig. 1. A sketch of a gas-liquid cylindrical cyclone separator showing the separator volumes, the pressure and liquid level and the inlet and outlet flows. The actual parabolic gas-liquid interface and the approximated gas-liquid interface are illustrated by solid and dashed lines, respectively.

i.e., the variable might be impossible to measure; or the available sensor technology might be unreliable, too difficult to maintain or simply too expensive.

Control of GLCC separators has been extensively studied in the literature. The proposed controllers either use few measurements, which are all available, or several measurements, some of which are unavailable. The first group of control algorithms typically require no model of the plant and therefore, they only achieve (feedback) control of the measured variables (e.g. [4], [5] and [6]). The last group of (advanced) controllers typically require a model of the plant and therefore, they achieve both (feedback and feed-forward) control of the measured variables and optimization based on unmeasured variables (e.g. [7], [8], [9], [10] and [11]). Information of these unmeasured variables are only available through estimation and require the development of estimators. A first attempt of state and parameter estimation of GLCC separators was proposed in [11], where a Model Predictive Controller (MPC) using state feedback from an Extended Kalman Filter (EKF) was derived. However, the EKF provided low robustness against measurement errors, due to inaccurate stochastic knowledge and prediction model, and was only capable of providing state feedback for approximately 1% measurement noise.

Generally, state and parameter estimation problems are either formulated using a deterministic or stochastic model of the plant, i.e., the modelling of the initial state and noises [12]. The objective of both estimators are, however, typically to minimize some squared error between the true states and the estimates states. The estimation problems are typically solved based on past data using recursive least-squares and differ only by addition of noise for the stochastic

estimation problems. Typical stochastic estimators are the Extended Kalman Filter (EKF) and the Unscented Kalman Filter (UKF), while a type of deterministic estimator is the Moving Horizon Estimator (MHE). The EKF and MHE are equivalent in least-squares sense for the case of an infinite estimation horizon and no active constraints. Details on these estimators are presented in Section IV.

To the authors' knowledge, little research focus on state and parameter estimation of GLCC separators, neither for enabling advanced controllers nor providing operators with necessary insight to efficiently operate the separator. Several types of stochastic and deterministic estimators exists, but only the EKF has been applied for state estimation of the GLCC separator. Therefore, in this paper, we derive and investigate the system performance of an UKF and a MHE providing state feedback to the linear output MPC proposed in [11]. A simplified model of the plant, consisting of two aggregated unknown parameters describing the separation performance, is derived to overcome the limited observability of the system. In contrast to [11], which assumed that states were directly measurable, albeit with noise, we use a nonlinear observation model mapping that maps from states to measurements. The UKF apply a nonlinear prediction and observation model of the plant. The MHE uses a linearized prediction model and a linear observation model, as the measurements used by the MHE are inverted prior to execution of the estimator. To reduce complexity and comply with industry standards, the MHE uses low-frequency measurements and high-frequency prediction, i.e., it uses software to compensate for imperfect hardware.

II. DYNAMIC MODEL

The GLCC separator is a centrifugal-based separator arranged as a vertically aligned cylindrical tank, illustrated in Fig. 1. The inlet gas-liquid flow w_{in} enters the separator tangentially, creating a rotational spin inside the separator. The high centrifugal forces created by the spinning motion separate the gas from the liquid due to their density difference. The gas accumulates in the upper part of the separator creating a gas pressure p_{G}, while the liquid accumulates at the bottom of the separator establishing a liquid level h_{L}. Because the separation inside the GLCC separator is incomplete, some liquid droplets will remain mixed with the accumulated gas, called wet gas (WG), and some gas bubbles will remain mixed with the accumulated liquid, called light liquid (LL). The accumulated gas and liquid are drained by the outlet flows w_{WG} and w_{LL}, respectively.

A dynamic model of the GLCC separator with initial separation of the inlet flow as developed in [6], and later extended with continuous separation of the accumulated gas and liquid volumes in [10]. We use this latter model in this paper, where the dynamics are described by the four ordinary differential equations (ODEs):

$$\begin{aligned}\dot{m}_{\text{LL,L}} =&(1-\beta_{\text{in}})w_{\text{in}} - \epsilon_{\text{in,L}}(1-\beta_{\text{in}})w_{\text{in}} \\ &+ \epsilon_{\text{L}}(1-\beta_{\text{WG}})m_{\text{WG,L}} - (1-\beta_{\text{LL}})w_{\text{LL}}\end{aligned} \tag{1}$$

$$\dot{m}_{\text{LL,G}} = \epsilon_{\text{in,G}}\beta_{\text{in}}w_{\text{in}} - \epsilon_{\text{G}}\beta_{\text{LL}}m_{\text{LL,G}} - \beta_{\text{LL}}w_{\text{LL}} \tag{2}$$

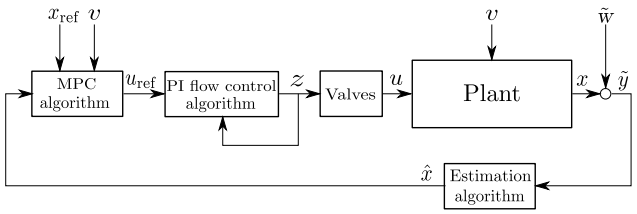

Fig. 2. A sketch of the closed-loop system.

$$\begin{aligned}\dot{m}_{\text{WG,L}} =&\epsilon_{\text{in,L}}(1-\beta_{\text{in}})w_{\text{in}} - \epsilon_{\text{L}}(1-\beta_{\text{WG}})m_{\text{WG,L}} \\ &- (1-\beta_{\text{WG}})w_{\text{WG}}\end{aligned} \tag{3}$$

$$\dot{m}_{\text{WG,G}} = \beta_{\text{in}}w_{\text{in}} - \epsilon_{\text{in,G}}\beta_{\text{in}}w_{\text{in}} + \epsilon_{\text{G}}\beta_{\text{LL}}m_{\text{LL,G}} - \beta_{\text{WG}}w_{\text{WG}}, \tag{4}$$

where the state $m_{\text{x,y}}$ is the mass of component y in x, $\beta_{\text{in}} \in [0,1]$ is the inlet gas mass fraction, $\beta_{\text{x}} \in [0,1]$ is the gas mass fraction in x, $\epsilon_{\text{in,y}} \in [0,1]$ is the immediate separation of component y at the inlet and $\epsilon_{\text{y}} \in [0,1]$ is the continuous separation of component y. The subscript x represents either inlet, WG or LL and the subscript y represents either G (gas) or L (liquid).

The gas mass fraction in the LL and WG are given by

$$\beta_{\text{LL}} = \frac{m_{\text{LL,G}}}{m_{\text{LL,G}} + m_{\text{LL,L}}} \tag{5}$$

$$\beta_{\text{WG}} = \frac{m_{\text{WG,G}}}{m_{\text{WG,G}} + m_{\text{WG,L}}}\,. \tag{6}$$

The dynamic model consists of two algebraic equations describing the liquid level and gas pressure given by

$$h_{\text{L}} = \frac{m_{\text{LL,L}} + m_{\text{LL,G}}}{a} \tag{7}$$

$$p_{\text{G}} = \frac{b m_{\text{WG,G}}}{aH - (m_{\text{LL,L}} + m_{\text{LL,G}})}\,, \tag{8}$$

where H is the total height of the tank and a and b are positive model parameters.

The outlet flows are determined by the opening percentage $z = [z_{\text{WG}}, z_{\text{LL}}]^\top$ of the respective control valves mounted on each of the outlets. The opening percentage to each of these control valves are controlled by two separate PI outlet flow controllers based on flow references generated by the MPC that constitute the manipulated variables for the control system.

III. CONTROL DESIGN

The linear MPC uses state feedback from an estimator and calculates the reference flows $u_{\text{ref}} = [u_{\text{LL,ref}}, u_{\text{WG,ref}}]^\top$ to the PI flow controllers controlling the outlet flows. The applied MPC controlling the level and pressure was presented in [11] and the following summary only includes the details necessary for the design of the estimators providing state feedback to the MPC. A block diagram of the closed-loop system is shown in Fig. 2.

The optimal control objective for the MPC is to track and stabilize the level and pressure at their respective references using a minimum number of changes in control inputs. The optimal control objective is mathematically described by a discrete-time Optimal Control Problem (OCP), structured as a Quadratic Programming (QP) problem, over a prediction horizon T_h. The QP problem is given as an objective function

J_{MPC} weighting deviations in states and control inputs from desired references x_{ref} and u_∞, respectively, subject to a linear prediction model. Optimal control is achieved by performing the following procedure, known as the MPC principle [13], at each time step k:

1) substitute recent estimates into the OCP,
2) solve the OCP to obtain an optimal control input sequence u^*,
3) apply the first vector element of u^* to the plant.

The MPC applies a transformed state-space model of (1)–(4) for prediction of the future behaviour of the system and to create a convex optimization problem with respect to the control variables. This mapping is a diffeomorphism on the operational region and is given by

$$x = T(m) = [h_{\text{L}},\, p_{\text{G}},\, m_{\text{LL,G}},\, m_{\text{WG,L}}]^\top, \tag{9}$$

where x is the transformed state vector and h_{L} and p_{G} is given by (7) and (8), respectively.

The fast dynamics of the plant (1)–(4) requires a fast sampling to capture the dynamics, but this sampling is too fast for industrial applications. Therefore, the MPC in [11] applies different sampling of states and control inputs for adaptation to industrial applications. The OCP is given by

$$\begin{aligned}\min_{u_{\text{ref}}} J_{\text{MPC}} = &\sum_{i=0}^{N} \frac{1}{||x_{\text{ref}}||_2^2}\big||x_i - x_{\text{ref},i}\big|\big|_Q^2 \\ &+ \sum_{i=0}^{N_u} \frac{1}{||u_{\infty,i}||_2^2}\big||u_i - u_{\infty,i}\big|\big|_R^2\end{aligned} \tag{10}$$

$$\text{s.t.} \quad x_0 = x_k \tag{11}$$

$$x_{\min} \le x_i \le x_{\max} \;\; \forall\, i \in \{0,\dots,N\} \tag{12}$$

$$u_{\min} \le u_i \le u_{\max} \;\; \forall\, i \in \{0,\dots,N_u\}, \tag{13}$$

where $Q \ge 0$ is the diagonal state weighting matrix, $R \ge 0$ is the diagonal control weighting matrix, $N = T_h/\Delta t_s$ is the state samples over T_h where Δt_s is the sampling time of the states, $N_u = T_h/T_u$ is the number of control input samples over T_h where Δt_u is the sampling time of the control inputs and the subscript max and min denotes upper and lower bounds. The notation $||z||_M = z^\top M z$ is used in this paper.

Offset-free control of the controlled variables h_{L} and p_{G} is achieved by augmenting the transformed state vector (9) with two integral error states of the controlled variables.

IV. ESTIMATOR DESIGN

The design of the UKF and the MHE are based on the transformed state vector x, and assuming limited-state knowledge of the plant. A comparison to an EKF was considered, but due to well-known weaknesses (specifically, it severely underestimates the covariance, regardless of tuning) in the estimator [14], the EKF would consistently diverge. These weaknesses were indeed why the UKF was initially invented. The level and pressure are the only measured states. In addition, the gas mass fractions of the two outlet flows β_{LL} and β_{WG} are measured. The inlet conditions w_{in} and β_{in} are considered known.

A. Estimation objective

The objective of the estimators are to estimate approximate values of the states and parameters, necessary for the MPC to control the plant based on the available measurements and statistical analysis.

B. Estimation model

Ideally, the estimators should apply the same transformed state-space model (9) as the MPC. This model consists of four states and four individual separation factors (unknown parameters). However, the available measurements only provide limited observability of the system and not enough information to estimate all states and parameters. Therefore, as in [11], the transformed state-space model (1)–(4) is simplified by describing the separation inside the separator using two unknown parameters and augmented the model with these as additional states. The resulting estimation model is given by

$$\dot{x}_1 = \frac{1}{a}\big[v_1 - \theta_1 + \theta_2 - w_{\text{LL}}\big] + w_1 \tag{14}$$

$$\begin{aligned}\dot{x}_2 = \frac{c_2}{a(H-x_1)}\Big[b\Big(v_2 - \theta_2 - \frac{a(x_2/c_2)(H-x_1)}{bx_4 + a(x_2/c_2)(H-x_1)} w_{\text{WG}} \\ + \Big(\frac{x_2}{c_2}\Big)\Big(v_1 - \theta_1 + \theta_2 - w_{\text{LL}}\Big)\Big] + w_2\end{aligned} \tag{15}$$

$$\dot{x}_3 = \theta_2 - \frac{x_3}{ax_1} w_{\text{LL}} + w_3 \tag{16}$$

$$\dot{x}_4 = \theta_1 - \frac{a(x_2/c_2)(H-x_1)}{bx_4 + a(x_2/c_2)(H-x_1)} w_{\text{WG}} + w_4 \tag{17}$$

$$\dot{\theta}_1 = w_5 \tag{18}$$

$$\dot{\theta}_2 = w_6, \tag{19}$$

where $w = [w_1, w_2, w_3, w_4, w_5, w_6]^\top \sim \mathcal{N}(0, W)$ is white process noise with covariance W disturbing the states, $v = [v_1, v_2]^\top$ is inlet flow and $\theta = [\theta_1, \theta_2]^\top$ is the unknown time-varying parameters. The variable x_2 is scaled from Pa to bar using the scaling variable $c_2 = 10^{-5}$.

The observation model is given by

$$\tilde{y} = \Big[x_1, x_2, \tfrac{x_3}{ax_1}, \tfrac{ax_2(H-x_1)}{ax_2(H-x_1)+bx_4}, 0, 0\Big]^\top + \tilde{v}, \tag{20}$$

where $\tilde{v} = [\tilde{v}_1, \tilde{v}_2, \tilde{v}_3, \tilde{v}_4, \tilde{v}_5, \tilde{v}_6]^\top \sim \mathcal{N}(0, \tilde{V})$ is white measurement noise with covariance V disturbing the measurements and $\tilde{y}$ is the measurements.

The nonlinear estimation model is compactly described by

$$\dot{\tilde{x}} = f(\tilde{x}(t), \tilde{u}(t)) + w \tag{21}$$

$$\tilde{y} = h(\tilde{x}(t)) + \tilde{v}, \tag{22}$$

where $\tilde{x} = [x, \theta]^\top$ is the augmented state vector, $\tilde{u} = [w, v]^\top$ is the augmented inputs, $f(\cdot)$ is the nonlinear prediction function comprising (14)–(19) and $h(\cdot)$ is the nonlinear observation function comprising (20).

C. Implementation

The plant model and the controller and estimators were implemented in MATLAB using CasADi version 3.1.0. CasADi is a software for solving numerical optimal control

problems using symbolic variables and algebraic differentiation, implemented in C++ with MATLAB wrappers [15]. The QP problems created by the MHE are solved using QPOASES, an open-source QP solver based on the active-set strategy [16].

The continuous-time nonlinear estimation model (21)–(22) is implemented symbolically using CasADi and used to calculate symbolic expressions of the discrete-time models, including exact algebraic derivatives. These symbolic expressions are calculated offline and evaluated numerically online by substituting symbolic variables for numerical values. This approach for calculation of the algebraic derivatives is both more accurate and less time consuming than calculating approximate numerical derivatives online.

D. Unscented Kalman Filter

The UKF is a stochastic nonlinear estimator that estimates the discrete-time augmented state vector $\tilde{x}_k$ using a discretized model of (21)–(22) as prediction and measurement model.

This discrete-time nonlinear estimation model is obtained from the continuous-time model (21)–(22), yielding the algebraic equations on the form

$$\tilde{x}_{k+1} = \tilde{f}(\tilde{x}_k, \tilde{u}_k) + w_k \tag{23}$$

$$\tilde{y}_k = h(\tilde{x}_k) + \tilde{v}_k\,, \tag{24}$$

where $\tilde{f}(\tilde{x}_k, \tilde{u}_k)$ is the discrete-time nonlinear prediction model, $w_k \sim \mathcal{N}(0, W\Delta t_s)$, $\tilde{v}_k \sim \mathcal{N}(0, V\Delta t_s)$, k is the time step, Δt is the sampling time and h is as in (22). The exact expression for $\tilde{f}$ is not explicitly found; the complexity of f and the unsuitability (in this case) of 1st-order Euler integration renders it impractical. Instead, the numerical integrator CVODES [17] was used. CVODES is an advanced numerical integrator that solves an initial value problem (IVP) using the variable step, variable order Backward Differentiation Formula (BDF) scheme and derivatives from CasADi to obtain the discrete-time dynamics at each discrete time sample.

The estimate retrieved by the UKF is modelled as a random variable, completely described by its mean $\hat{x}_k$ and error covariance P_k. The estimate at time k is calculated through a two-step procedure: first by a prediction step and subsequently by a correction step. The prediction step estimates the *a priori* estimate $\hat{x}_k^-$ and P_k^- based on the previous *a posteriori* estimate $\hat{x}_{k-1}^+$ and P_{k-1}^+ using a discrete-time nonlinear prediction model. The correction step estimates the a posteriori estimate $\hat{x}_k^+$ and P_k^+ based on $\hat{x}_k^-$ and P_k^- and the recent measurement $\tilde{y}_k$ using the measurement model (20) and the Kalman gain K_k.

The UKF is an improvement of the EKF and is based on the principle that an approximation of the random variable properties based on a set of transformed points is more correct than an estimate of the random variable properties based on a single point [14]. This estimation approach achieves provably increased accuracy of the estimates $\hat{x}_k$ and P_k compared to the EKF with the downside of increased computational cost [14]. The UKF chooses two sets of sigma points for each of the estimation steps. The set of sigma points $\mathcal{X}_{k-1}$ whose elements are time-propagated using the discrete-time nonlinear prediction model in the prediction step is based on $\hat{x}_{k-1}^-$ and P_{k-1}^-. The set of sigma points $\mathcal{X}_k$ whose elements are transformed to measurements using the discrete-time nonlinear observation model in the correction step is based on $\hat{x}_k^+$ and P_k^+. The statistical properties of the estimates in each of the estimation steps are then approximated as the sample mean of the propagated sigma points. The sigma points are chosen according to the distribution

$$\mathcal{X}_{i,k} = \begin{cases} \hat{x}_k^\star + \left(\sqrt{nP_k^\star}\right)_i & \forall\, i = 1, \ldots, n \\ \hat{x}_k^\star - \left(\sqrt{nP_k^\star}\right)_i & \forall\, i = 1+n, \ldots, 2n\,, \end{cases} \tag{25}$$

where $\mathcal{X}_{i,k}$ is ith sigma points at time k in the set of sigma points $\mathcal{X}_k$, n is the dimension of $\hat{x}_k$, $\sqrt{nP_k^\star}_i$ is the ith row of $\sqrt{nP_k^\star}$ and $\star$ represents either a priori estimate $(-)$ or a posteriori estimate $(+)$.

The implemented UKF is based on [18, Ch. 14], [19] and [20] and the pseudo code is shown in Algorithm 1.

Algorithm 1 UKF

Require: Input: $\tilde{y}_k$, $\hat{x}_{k-1}$, $\tilde{u}_{k-1}$, P_{k-1}^+, W, V

PREDICTION STEP

Choose $\mathcal{X}_{k-1}$ according to (25) using $\hat{x}_{k-1}^+$ and P_{k-1}^+

Calculate $\mathcal{X}_{i,k} = \tilde{f}(\mathcal{X}_{i,k-1}, \tilde{u}_{k-1})$

Update $\hat{x}_k^- = \frac{1}{2n}\sum_{i=1}^{2n} \mathcal{X}_{i,k}$

Update $P_k^- = \frac{1}{2n}\sum_{i=1}^{2n} ||\mathcal{X}_{i,k} - \hat{x}_k^-||^2 + W$

CORRECTION STEP

Choose $\mathcal{X}_k$ according to (25) using $\hat{x}_k^-$ and P_k^-

Calculate $\mathcal{Y}_{i,k} = h(\mathcal{X}_{i,k})$

Update $\hat{y}_k = \frac{1}{2n}\sum_{i=1}^{2n} \mathcal{Y}_{i,k}$

Calculate K_k using $\mathcal{X}_k$, $\hat{x}_k^-$, $\mathcal{Y}_k$, $\hat{y}_k$ and V

Update $\hat{x}_k^+ = \hat{x}_k^- + K_k(\tilde{y}_k - \hat{y}_k)$

Update $P_k^+ = P_k^- - K_k\left(\frac{1}{2n}\sum_{i=1}^{2n} ||\mathcal{Y}_{i,k} - \hat{y}_k||^2 + V\right)^{-1} K_k^\top$

return $\hat{x}_k = \hat{x}_k^+$ and P_k^+

E. Moving Horizon Estimator

The linear MHE is a deterministic estimator that estimates the discrete-time augmented state vector $\tilde{x}_k$ modelled as a deterministic variable using a discrete-time linear estimation model that approximates (21)–(22).

The measurements used by the MHE are pre-inverted prior to execution of the estimator resulting in a linear relationship between the measurements and the estimated states. The discrete-time linear prediction model that linearly approximates (21) is obtained by first linearizing and then discretizing with time sampling Δt_s yielding

$$\tilde{x}_{k+1} = \frac{\mathrm{d}f}{\mathrm{d}\tilde{x}}\Big|_{\tilde{x}=\tilde{x}_k} \tilde{x} + \frac{\mathrm{d}f}{\mathrm{d}\tilde{u}}\Big|_{\tilde{u}=\tilde{u}_k} \tilde{u} + w_k = A_k\tilde{x} + B_k\tilde{u} + w_k \tag{26}$$

$$y_k = h^{-1}(\tilde{y}_k) \approx h^{-1}(h(\tilde{x}_k)) + v_k = \tilde{x}_k + v_k\,, \tag{27}$$

where y_k is the discrete-time transformed measurements, $v_k = [v_{1,k}, v_{2,k}, v_{3,k}, v_{4,k}, v_{5,k}, v_{6,k}]^\top \sim \mathcal{N}(0, V)$ is white measurement noise with constant covariance V, A_k is

the continuous-time Jacobian of the states and B_k is the continuous-time Jacobian of the inputs.

The MHE is based on solving an Optimal Estimation Problem (OEP) using observations of measurements and inputs on a finite moving time window in the past to estimate the current discrete-time augmented state vector $\tilde{x}_k$ that best fits these measurements. The OEP is structured as a QP problem based on the available information gathered in the information vector ι_k. The QP problem is specified by an objective function J_{MHE} weighting the changes in state predictions and deviations in predicted observations from past measurements subject to the discrete-time linear estimation and observation model. Optimal estimation of the defined OEP[1] is achieved by performing a procedure similar to the MPC principle, which we call the MHE principle, at each time step k:

1) substitute past observations into the OEP,
2) solve the OEP to obtain the an estimate $\hat{x}_k$ of $\tilde{x}_k$,
3) make the recent $\hat{x}_k$ available to other applications including the controller.

As for the MPC, the prediction horizon needs to be sufficiently long to allow the system dynamics to change and thereby ensure feasibility. The sampling of the system dynamics is much faster than any industrial application is able to sample measurements and change the inputs. Therefore, to reduce complexity and comply for use in industrial applications, the MHE operates with a sampling time equal to the sampling of the observations, while the sampling time of the state predictions Δt_s is much faster. The information vector is given by

$$\begin{aligned}\iota_k = [&y_{k-N+N_x},\, \ldots,\, y_{k-N+N_yN_x},\\ &\tilde{u}_{k-N},\, \ldots,\, \tilde{u}_{k-N+(N_y-1)N_x}],\end{aligned} \tag{28}$$

where $N = T_h/\Delta t_s$ is the moving window horizon, T_h is the time horizon of the moving window, $N_y = T_h/\Delta t_y$ is the number of gathered observations where Δt_y is the sampling time of the observations and $N_x = N/N_y = \Delta t_y/\Delta t_s$ is the number of states predictions between each observation sample.

The OEP can be compactly written using an objective function given as the weighting sum of the process and measurement noises subject to the discrete-time linear estimation and observation model. The linear prediction is updated for each measurement sampling over the moving window horizon to increase their accuracy creating a scheduling MHE. The OEP assumes knowledge of the first a posteriori estimate $\hat{x}_{k-N} = \hat{x}^+_{k-N}$ that is determined using the discrete-time linear estimator model (26) and the previous a posteriori estimate $\hat{x}_{k-N-1-N_x} = \hat{x}^+_{k-N-1-N_x}$. Additionally, the MHE requires an initial guess of the estimates $\hat{X}^-_k = [\hat{x}^-_{k-N}, \ldots, \hat{x}^-_k]^\top$ for solving the OEP. This initial guess is actually the a priori estimates and is calculated by time shifting the previous a posteriori estimates $\hat{X}^+_{k-1}$ one time step forward in time. The OEP is solved by substituting the constraints into the objective function and the solution is the a posteriori estimates $\hat{X}_k = \hat{X}^+_k = \tilde{X}_k$. The last element of $\hat{X}_k$ contains the current discrete-time estimate that is provided to other applications. The compactly written OEP is given by

$$\begin{aligned}\min_{\tilde{x},\mathrm{v},\mathrm{w}}\ J_{\text{MHE}} = &\left|\left|\hat{x}_{k-N} - \tilde{x}_{k-N}\right|\right|^2_{S^{-1}} + \sum_{i=1}^{N_y} \left|\left|v_{k-N+iN_x}\right|\right|^2_{V^{-1}}\\ &+ \sum_{i=1}^{N_y}\sum_{j=0}^{N_x-1} \left|\left|w_{k-N+(i-1)N_x+j}\right|\right|^2_{W^{-1}}\end{aligned} \tag{29}$$

$$\text{s.t.}\quad \hat{x}_{k-N} = A_{\mathrm{d},k-N}\hat{x}_{k-N-1-N_x} + B_{\mathrm{d},k-N}\tilde{u}_{k-N-1-N_x} \tag{30}$$

$$\begin{aligned}\tilde{x}_{k-N+1+i} = &A_{\mathrm{d},k-N+jN_x}\tilde{x}_{k-N+i}\\ &+ B_{\mathrm{d},k-N+jN_x}\tilde{u}_{k-N+jN_x} + w_{k-N+i}\\ &\forall\, i \in \{k-N, \ldots N-1\},\ j \in \{1, \ldots N_y\}\end{aligned} \tag{31}$$

$$\begin{aligned}y_{k-N+iN_x} = &\tilde{x}_{k-N+iN_x} + v_{k-N+iN_x}\\ &\forall\, i \in \{1, \ldots N_y\}\end{aligned} \tag{32}$$

$$x_{\min} \le \tilde{x}_i \le x_{\max} \quad \forall\, i \in \{k-N, \ldots N\}, \tag{33}$$

where $W \ge 0$ is the diagonal state prediction weighting matrix expressing the confidence in the state prediction, $V \ge$ is the diagonal predicted observation weighting matrix expressing the confidence in the past measurements, and $S \ge 0$ is the diagonal arrival cost weighting matrix indicating the importance of the discarded information before the start if the moving time window.

The implemented MHE is based on [21, Ch. 4], [22] and [12] and the pseudo code is shown in Algorithm 2.

Algorithm 2 MHE

Require: Input: $\hat{x}_{k-N-1-N_x}, \tilde{u}_{k-N-1-N_x}, \iota_k, \hat{X}_{k-1}, S, W, V$
1: **if** mod(time, Δt_y) == 0 **then**
2: Invert measurements using $h^{-1}(\tilde{x}_k)$
3: Update linear the Jacobian matrices A_{d} and B_{d}
4: Update $\hat{X}^-_k$ by time shifting $\hat{X}^+_{k-1}$
5: Update and solve QP (29)–(33) to obtain $\hat{x}^+_k = \tilde{x}_k$
6: **return** $\hat{x}_k = \hat{x}^+_k$
7: **else**
8: **return** $\hat{x}_{k-1}$

TABLE I
SIMULATION AND TUNING PARAMETERS.

Parameters	Value	Unit
Q	$\mathrm{diag}[8000; 8000; 0; 0; 1000; 1000]^\top$	-
R	$\mathrm{diag}[200; 200]^\top$	-
T_h	10	s
Δt_u	1	s
Δt_y	1	s
Δt_s	0.05	s
W_{UKF}	$\mathrm{diag}[0.001, 0.01, 0.001, 0.01, 0.001, 0.0001]^\top$	-
V_{UKF}	$\mathrm{diag}[0.001, 0.1, 0.01, 0.01]^\top$	-
S_{MHE}	$\mathrm{diag}[1, 10^{-6}, 1, 10^{-6}, 10^{-8}, 10^{-8}]^\top$	-
W_{MHE}	$\mathrm{diag}[0.001, 0.05, 0.001, 0.01, 0.0001, 0.00001]^\top$	-
V_{MHE}	$\mathrm{diag}[0.001, 0.001, 0.1, 0.1]^\top$	-
$x_{\min}$	$[h_{\text{L,min}}, p_{\text{G,min}}, -\infty, -\infty, -\infty, -\infty]^\top$	-
$x_{\max}$	$[h_{\text{L,max}}, p_{\text{G,max}}, \infty, \infty, \infty, \infty]^\top$	-

[1]Optimal estimation is usually defined as optimization of the full information problem, but optimization of the OEP yields the optimal estimate for this problem.

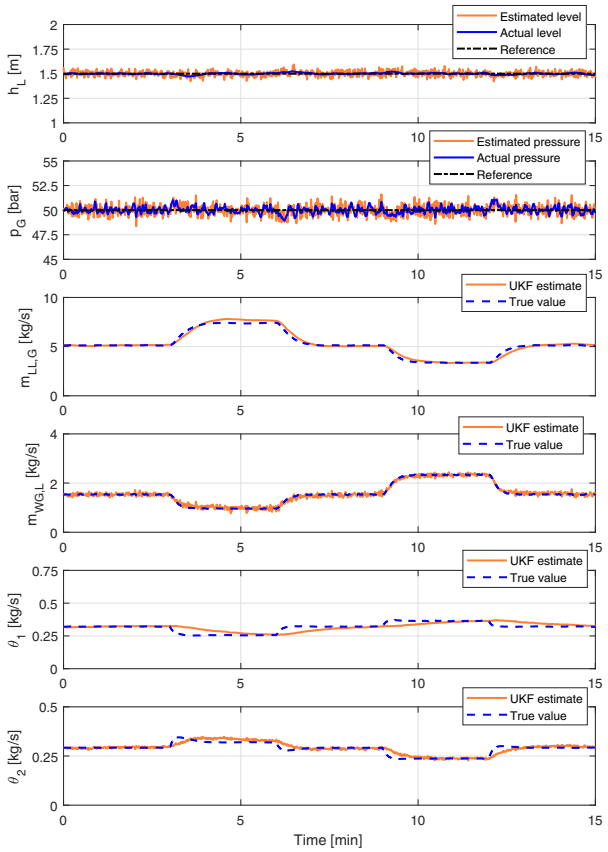

Fig. 3. Performance of the MPC using state feedback from the UKF.

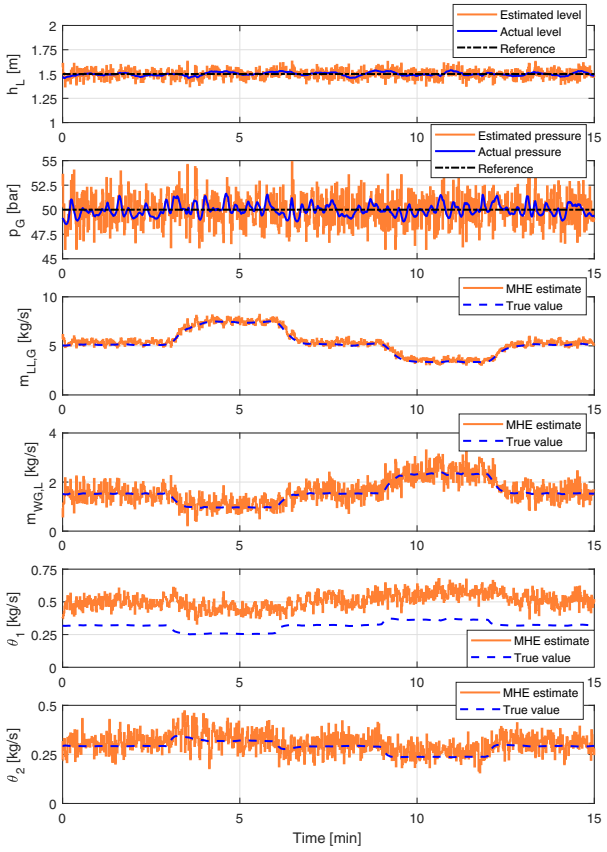

Fig. 4. Performance of the MPC using state feedback from the MHE.

F. Tuning

The estimation performance of the UKF and MHE depend on the tuning of the diagonal covariance matrices W and V. A small diagonal element on W implies confidence in the estimator model for the corresponding state estimate, while a large diagonal value on V implies less confidence in the corresponding measurement. The additional arrival cost term S of the MHE weights the importance of the discarded observations before the moving time window and a large diagonal element implies confidence in the earliest state predictions and thereby slower convergence rate.

The simulations were performed using different constant covariance matrices for each of the estimators. These covariance matrices were, based on the insight explained above, individually tuned by trial-and-error until satisfactory performance was achieved. The applied covariance matrices and other simulation parameters are listed in Table I.

V. SIMULATIONS AND DISCUSSION

The estimators were studied individually in simulations for the same inlet conditions and measurement noises. The inlet conditions comprise the inlet flow w_{in} and the inlet gas mass fraction β_{in}. The inlet flow, a mixture of gas and liquid, changes every 3 minutes over a total simulation time of 15 minutes between a low, intermediate and high gas mass fraction inlet flow to analyse estimation performance at extreme inlet conditions. Physical parameters and properties of 25° API crude oil at 50 bar and 30°C similar to [11] are used for the simulations.

Additive band-limited zero-mean Gaussian white noise was added to all measurements available for the estimators. The variance of this noise is given by $\sigma_z^2 = (A_z \mu_z)^2$ where σ_z is the standard deviation of measurement z, A_z is the white-noise variation of z and μ_z is the mean nominal value of z. The mean nominal values are determined offline on the basis of expected deviations from normal operation (nominal operation) and are listed in Table II. The performance of the MPC using state feedback from the individual estimators is shown in Figs. 3–4.

A performance measure for each of the separate units and the closed-loop system is required to objectively evaluate their performance. Defining the estimator error as $e = \hat{x} - \tilde{x}$, the estimator objective is to obtain unbiased estimates ($\text{E}[e] = 0$) with minimum variance, i.e., minimizing $\text{E}[(e - \text{E}[e])]$. The control objective is to achieve tracking of the controlled variable references based on recent state estimates, i.e., minimizing the control error $e_{\text{ctrl}} = \hat{x} - \tilde{x}_{\text{ref}}$.

TABLE II

STATISTICAL NOISE PROPERTIES.

A_z[%]	$\mu_{w_{\text{in}}}$[kg/s]	$\mu_{\beta_{\text{in}}}$[-]	$\mu_{h_{\text{L}}}$[m]	$\mu_{p_{\text{G}}}$[bar]	$\mu_{\beta_{\text{LL}}}$[-]	$\mu_{\beta_{\text{WG}}}$[-]
3.00	12.40	0.23	1.50	50.00	0.05	0.85

TABLE III

RMS VALUES FOR THE CONTROL AND CLOSED-LOOP SYSTEM ERRORS.

RMS value	Control ($\hat{x} - \tilde{x}_{\text{ref}}$)		System ($\tilde{x} - \tilde{x}_{\text{ref}}$)	
	UKF	MHE	UKF	MHE
h_{L}	0.0281	0.0475	0.0095	0.0188
p_{G}	0.6101	1.6317	0.4627	0.6899

The performance of the closed-loop system combines the objective of both the estimator and controller specified by minimizing the system error $e_{\text{sys}} = \tilde{x} - \tilde{x}_{\text{ref}}$. The performance of the controller and the closed-loop system are evaluated using RMS values of e_{ctrl} and e_{sys} for the controlled variables as shown in Table III. Since the estimators are based on a statistical analysis, their performance are evaluated using statistical properties (mean and variance) of $e = \hat{x} - \tilde{x}$ for all estimation variables as shown in Table IV.

The simulations show that the state feedback MPC is able to control the plant using state feedback from both the UKF and the MHE. The MPC using state feedback from the UKF achieves excellent tracking of both the level reference $h_{\text{L,ref}}$ and the pressure reference $p_{\text{G,ref}}$ with no significant transients upon changes in inlet conditions and only minor oscillations around the references. The MPC using state feedback from the MHE achieves good tracking of $h_{\text{L,ref}}$ with no significant transients upon changes in inlet conditions, but with larger oscillations around the references. A general observation of the estimator performances indicate that the UKF generally achieves better estimates of all estimated states, but with larger convergence rate to the true values than MHE.

The UKF uses a nonlinear prediction and observation model of the plant, while the MHE uses a linear prediction and observation model of the plant. The nonlinear models provide significantly higher accuracy over the linear models at the expense of increased computational load.

A close observation of the RMS values measuring the control performance of the level reveal that the average control error using state feedback from the UKF is slightly smaller than using state feedback from the MHE. The RMS values measuring the control performance of the pressure show that the average control error using state feedback from the UKF is significantly smaller than using state feedback from the MHE. As expected, equivalent observations are obtained by comparing system performance for both estimators, but with smaller errors for the measured variables.

A general observation of the statistical properties for the different estimators show that the UKF achieves the best estimates, having the smallest error mean (bias) and error variance. The statistical properties of the estimates show that both estimators achieve good estimates of the level with small bias and error variance. However, only the UKF achieves good pressure estimates with small bias and error variance. The MHE achieves acceptable pressure estimates with compressed measurement noise. Again the UKF achieves good estimates of $m_{\text{LL,G}}$ and $m_{\text{WG,L}}$. The MHE achieves good estimates of $m_{\text{LL,G}}$ with small bias and error variance, but only acceptable estimates of $m_{\text{WG,L}}$ with small bias and significant error variance. Also for the parameter estimates θ_1 and θ_2, the UKF achieves the best estimates with small bias and error variance. The MHE achieves acceptable estimates of θ_2 with small bias and significant error variance, but poor estimates of θ_2 with significant bias and error variance.

TABLE IV

STATISTICAL PROPERTIES FOR THE ESTIMATOR ERRORS.

Statistical properties	Mean $(\bar{e} = E[e])$ UKF	MHE	Variance $(\sigma_e^2 = E[(e-\bar{e})^2])$ UKF	MHE
h_{L}	-0.0075	-0.0014	0.0006	0.0016
p_{G}	0.0469	-0.0594	0.1382	1.8256
$m_{\text{LL,G}}$	0.1058	0.1510	0.1323	0.0457
$m_{\text{WG,L}}$	0.0077	0.0723	0.0029	0.0796
θ_1	-0.0008	0.1929	0.0002	0.0018
θ_2	0.0043	0.0043	0.0003	0.0016

The significant pressure oscillations experienced by the MPC using state feedback from the MHE are likely to be caused by the variation in the $m_{\text{WG,L}}$, θ_1 and θ_2 which significantly affects the pressure dynamics. These variations are severe enough to render the prediction model of the MPC inaccurate and thus reduce the quality of the control inputs, causing the pressure oscillations.

VI. CONCLUSIONS

In this paper, a nonlinear UKF and a linear MHE estimators were designed for estimating unmeasured states and unknown parameters of a GLCC separator. The MHE pre-inverts the measurements before execution and uses a linear prediction model and observation model. In contrast, the UKF uses a nonlinear prediction model for state prediction and the nonlinear observation function. The MHE used a different sampling time of the state predictions and observations, and the optimization problem was solved using an interior point solver.

The performance of the estimators were studied in separate simulations for the same inlet conditions providing state feedback to a linear output control MPC. The estimator performances were evaluated based on statistical properties of the estimates, while the control and system performances were evaluated by RMS values. The UKF was able to accurately predicting both unknown parameters without any bias, while the MHE was only able of accurately predicting one parameter without bias and the other with significant bias.

Generally, the MPC using state feedback from the UKF achieved better control performance than using state feedback from the MHE. Especially the pressure experienced larger oscillations using state feedback from the MHE. These oscillations are probably due to larger error variations in the estimates of the gas dynamics ($m_{\text{WG,L}}$, θ_1 and θ_2), which propagates through the MPC and causes the control input to oscillate.

The UKF performs better than the MHE because it uses a nonlinear prediction model, but the improved performance comes at the cost of increased computational load. However, considering the relatively small deviations in system performance when using the MHE, the linear MHE is an interesting compromise.

The main difference between the UKF and the MHE is that the UKF uses a nonlinear model, while the MHE uses a linear model. As this study has shown, this difference is significant, especially for estimation of the pressure and accurate prediction of both unknown parameters. The estimation performance is likely to improve using a nonlinear prediction and observation model for the MHE and this is left as future work.

ACKNOWLEDGMENTS

This project is supported by the Norwegian Research Council, industrial partners and NTNU under the Subsea Production and Processing (SUBPRO) SFI program.

REFERENCES

[1] A. Hannisdal, R. Westra, M. R. Akdim, A. Bymaster, E. Grave, and D. Teng, "Compact separation technologies and their applicatbility for subsea field development in deep water," in *Offshore technology conference*, 2012.

[2] O. Kristiansen, Ø. Sørensen, and O. R. Nilssen, "Compactsep– compact subsea gas-liquid separator for high-pressure wellstream boosting," in *Offshore Technology Conference*, 2016.

[3] G. E. Kouba, S. Wang, L. E. Gomez, R. S. Mohan, and O. Shoham, "Review of the state-of-the-art gas-liquid cylindrical cyclone (GLCC) technology-field applications," in *International Oil & Gas Conference and Exhibition in China*, 2006.

[4] S. Wang, R. S. Mohan, O. Shoham, and G. E. Kouba, "Dynamic simulation and control system design for gas-liquid cylindrical cyclone separators," *SPE Annual Technical Conference and Exhibition*, 1998.

[5] S. Wang, R. Mohan, O. Shoham, J. D. Marrelli, and G. E. Kouba, "Optimal control strategy and experimental investigation of gas-liquid compact separators," *SPE Annual Technical Conference and Exhibition*, 2000.

[6] T. T. Kristoffersen, C. Holden, S. Skogestad, and O. Egeland, "Control-oriented modelling of a gas-liquid cylindrical cyclone," in *Proceedings of the American Control Conference*, 2017.

[7] M. Leskens, A. Huesman, S. Belfroid, P. Verbeek, A. Fuenmayor, P. M. J. V. den Hof, E. Nennie, and R. Henkes, "Fast model based approximation of the closed-loop performance limits of gas/liquid inline separators for accelerated design." in *Proceedings of the 18th IFAC World Congress*, 2011.

[8] T. T. Kristoffersen, C. Holden, and O. Egeland, "Feedback linearizing control of a gas-liquid cylindrical cyclone," in *Proceedings of the 20th World Congress of the Internation Federation of Automatic Control*, 2017.

[9] S. J. Ohrem, T. T. Kristoffersen, and C. Holden, "Adaptive feedback linearizing control of a gas-liquid cyclindrical cyclone," in *Proceedings of the 1st IEEE Conference on Control Technology and Applications*, 2017.

[10] T. T. Kristoffersen and C. Holden, "Nonlinear model predictive control of a gas-liquid cylindrical cyclone," in *Proceedings of the 25th Mediterranean Conference on Control and Automation*, 2017.

[11] ——, "Model predictive control and extended Kalman filter for a gas-liquid cylindrical cyclone," in *Proceedings of the 1st IEEE Conference on Control Technology and Applications*, 2017.

[12] A. Alessandri, M. Baglietto, and G. Battistelli, "Receding-horizon estimation for discrete-time linear systems," *IEEE Transactions on automatic control*, 2003.

[13] J. M. Maciejowski, *Predictive Control with Constraints*. Pearson Education Limited, 2002.

[14] S. J. Julier and J. K. Uhlmann, "Unscented filtering and nonlinear estimation," *Proceedings of IEEE*, 2004.

[15] J. Andersson, J. Åkesson, and M. Diehl, "CasADi – a symbolic package for automatic differentiation and optimal control," in *Recent Advances in Algorithmic Differentiation*, 2012.

[16] H. J. Ferreau, C. Kirches, A. Potschka, H. G. Bock, and M. Diehl, "qpOASES: a parametric active-set algorithm for quadratic programming," *Mathematical Programming Computation*, 2013.

[17] A. C. Hindmarsh and R. Serban, *User documentation for CVODES v3.1.0*, nov 2017.

[18] D. Simon, *Optimal state estimation*. Wiley, 2006.

[19] S. Kolås, B. A. Foss, and T. S. Schei, "Constrained nonlinear state estimation based on the UKF approach," *Computers and chemical engineering*, 2009.

[20] R. Kandepu, B. Foss, and L. Imsland, "Applying the unscented Kalman filter for nonlinear state estimation," *Journal of process control*, 2008.

[21] J. B. Rawlings and D. Q. Mayne, *Model Predictive Control: Theory and Design*. Nob Hill Publishing, 2015.

[22] D. Sui, T. A. Johansen, and L. Feng, "Linear moving horizon estimation with pre-estimating observer," *IEEE Transactions on automatic control*, 2010.